PCMDI

Program for Climate Model Diagnosis and Intercomparison

UCRL-ID-122565

PCMDI Report No. 30

CORRELATION BETWEEN OUTGOING LONGWAVE RADIATION AND SURFACE TEMPERATURE IN THE TROPICAL PACIFIC: A MODEL INTERCOMPARISON

by

Curt Covey

Program for Climate Model Diagnosis and Intercomparison
Lawrence Livermore National Laboratory, Livermore, CA, USA

January 1996

PROGRAM FOR CLIMATE MODEL DIAGNOSIS AND INTERCOMPARISON
UNIVERSITY OF CALIFORNIA, LAWRENCE LIVERMORE NATIONAL LABORATORY
LIVERMORE, CA 94550

DISCLAIMER

This document was prepared as an account of work sponsored by an agency of the United States Government. Neither the United States Government nor the University of California nor any of their employees, makes any warranty, express or implied, or assumes any legal liability or responsibility for the accuracy, completeness, or usefulness of any information, apparatus, product, or process disclosed, or represents that its use would not infringe privately owned rights. Reference herein to any specific commercial product, process, or service by trade name, trademark, manufacturer, or otherwise, does not necessarily constitute or imply its endorsement, recommendation, or favoring by the United States Government or the University of California. The views and opinions of authors expressed herein do not necessarily state or reflect those of the United States Government or the University of California, and shall not be used for advertising or product endorsement purposes.

This is an informal report intended primarily for internal or limited external distribution. The opinions and conclusions stated are those of the author and may or may not be those of the Laboratory.

This report has been reproduced
directly from the best available copy.

Available to DOE and DOE contractors from the
Office of Scientific and Technical Information
P.O. Box 62, Oak Ridge, TN 37831
Prices available from (615) 576-8401, FTS 626-8401

Available to the public from the
National Technical Information Service
U.S. Department of Commerce
5285 Port Royal Rd.,
Springfield, VA 22161

ABSTRACT

Results from the Atmospheric Model Intercomparison Project show that general circulation models tend to underestimate the emission of anomalous heat to space during the 1987 El Niño episode in the tropical Pacific. This bias suggests that the models may underestimate negative feedbacks on climate involving longwave radiation in the tropical atmosphere. Such a possibility is consistent with analyses of paleo-data that suggest climate models generally overestimate climate sensitivity in the tropics.

1. Introduction

A recent paper by M.-D. Chou (1994) provides observational data that may be related to Earth's climate sensitivity (e.g., global changes expected from human production of carbon dioxide, aerosols, etc.). Using the Earth Radiation Budget Experiment data set, Chou examined the correlation between outgoing radiation at the top of the atmosphere and changes in climate during an El Niño episode. He concluded that his "results are consistent with [R. S.] Lindzen's hypothesis that reduced upper-tropospheric water vapor in the vicinity of the enhanced convection region produces cooling that counteracts warming in the Tropics." Lindzen (1990, 1994) has used this hypothesis to argue against the idea that positive water-vapor feedback amplifies the sensitivity of the climate. Chou's observations may thus pose a challenge to conventional-wisdom estimates of future global warming such as those given by the Intergovernmental Panel on Climatic Change (Houghton et al., 1990).

The simplest quantitative perspective on this controversy is obtained by considering a hypothetical planet radiating to space as a blackbody with uniform surface temperature T (Hansen et al., 1981). Suppose the rate of energy input to the surface-atmosphere system increases by ΔQ Watts per square meter. The temperature would then increase to a new equilibrium value given by $\Delta(\sigma T^4) = \Delta Q$, where σ is the Stefan-Boltzmann Constant. For a doubling of atmospheric CO_2, $\Delta Q \sim 4$ W m^{-2} (Houghton et al., 1990). Using $T \sim 255$ K (the effective radiating temperature of Earth), one obtains $\Delta T \sim 1$ K. General circulation models, however, typically obtain globally averaged ΔT values considerably in excess of 1 K after CO_2 doubling. In the models, atmospheric water vapor increases as global temperatures rise. Increased water vapor, in turn, adds to the greenhouse trapping of outgoing longwave radiation. This positive water-vapor feedback enhances the original warming.

Chou's analysis related (among other things) changes in outgoing longwave radiation at the top of the atmosphere and changes in surface temperature, during natural fluctuations of the climate. His results apply only to the tropical Pacific (30°S-30°N, 100°E-100°W). Changes in globally averaged OLR and globally averaged surface temperatures are too small during interannual climate fluctuations to form a reliable correlation. In the tropical Pacific, however, large changes in OLR and sea surface temperature are associated with the El Niño phenomenon. Chou compared an El Niño time, April 1987, to a non-El Niño time, April 1985. He found that area-averaged tropical Pacific SST was 0.3 K warmer, and area-averaged tropical Pacific OLR was 6.8 W m^{-2} greater, at the El Niño time. But substituting T ~ 300 K into $4\sigma T^3 \times (0.3\ K)$ gives less than 2 W m^{-2}. One may conclude that the real tropical Pacific atmosphere rejects the excess surface heat of El Niño to space more readily than a simple blackbody model would suggest—rather than less readily, as might be expected under the hypothesis of positive water vapor feedback.

The relationship between the mechanisms responsible for OLR changes in El Niño and the mechanisms operating in longer-term global changes, such as global warming, are no doubt complex. It is not my purpose here to investigate that relationship. Nevertheless, a natural question arising from Chou's observations is: to what extent are atmospheric GCMs able to reproduce them? That is the subject of this Note.

2. AMIP model results

The Atmospheric Model Intercomparison Project (Gates, 1992) provides a data base of output from 30 atmospheric GCMs run under identical boundary conditions. The boundary conditions include monthly mean SSTs observed for the period 1979-1988, covering the time periods examined by Chou. Of the 30 AMIP models, 29 include OLR in their output. I have examined the changes in tropical Pacific OLR between April 1985 and April 1987 for these 29 models, and I summarize the results in Table 1 and Figure 1. OLR arising from the combination of clear and cloudy skies that a model simulates in the normal course of its integration is hereinafter designated "total-sky OLR." In addition, I include for 13 models the OLR arising from only the clear-sky portions of each area element. I obtained the models' clear-sky OLR from cloud radiative forcing calculated by Potter and Fiorino (1995). The Table and Figure also include the observed total-sky and clear-sky numbers from ERBE.

The first and last columns of the Table show averages over the same domain that Chou considered: 30°S-30°N, 100°E-100°W. For this domain, the average change (April 1987 minus April 1985) in total-sky tropical Pacific OLR for the models is 3.4 W m^{-2}, about half the value observed. (The observed value given in the Table is 3% different from Chou's, apparently because I included land as well as ocean areas in the domain.) The standard deviation of the model total-sky values is 2.9 W m^{-2}. For clear-sky data, the model-average change in OLR is 2.3 W m^{-2}, between two-thirds and three-fourths the value observed, and the standard deviation is 1.3 W m^{-2}. For both total- and clear-sky data, application of standard "twice-sigma" error bars to the model average would produce a range that includes the observed value in the range of model results. There seems little doubt, however, that the models exhibit a systematic bias of not enough increase in OLR. This point is made by Figure 1, a histogram of the results shown in Table 1. For total-sky data, all models except one obtain Δ(OLR) values less than observed. Note that the one model obtaining greater total-sky Δ(OLR) values than observed gets values far in excess of observations. The extreme positions of such "outliers" do not affect the model-*median* total-sky and clear-sky Δ(OLR) values. These are even smaller than the models' mean values: 2.9 and 1.8 W m^{-2} for total- and clear-sky respectively. A related statistic, also implying a systematic model underestimate of Δ(OLR), is the following: among the models, 18 of 29 get less than half the total-sky value observed, and 6 of 13 get less than half the clear-sky value observed.

Error limits in the ERBE observations introduce an additional uncertainty in the analysis. This uncertainty does not appear great enough to reverse the conclusions implied above, however. Barkstrom (1984) estimated 10 W m^{-2} ERBE OLR errors for monthly mean grid points at 2.5° resolution. If these errors combine randomly over the area 30°S-30°N, 100°E-100°W, which contains nearly 1600 such grid points, then the error in the averages discussed above is about $10 / (1600)^{1/2} = 0.25$ W m^{-2}. This number is far smaller than the systematic difference between models and observations that is evident in Figure 1. If the ERBE point-errors combine systematically, then errors in the averages up to 10 W m^{-2} are possible, but it is not obvious where such correlated errors would come from in the total-sky observations. This remark applies especially to the present work, which is concerned only with *differences* between two sets of observations, so that many kinds of systematic error would cancel. For clear-sky observations the situation is complicated by differing definitions in models and observations. The models define clear-sky fluxes at all grid points by simply redoing their radiation transport calculations without clouds present. ERBE, on the other hand, defines clear-sky fluxes only at grid points that are actually free of clouds. In the tropics, models would thus include clear-sky fluxes from areas with deep convection and high water-vapor concentrations, which were omitted in the ERBE data-processing. Inclusion of these areas in the model's output would result in an "underestimate" of clear-sky OLR compared to ERBE. It is not clear what effect this inconsistency has on the *differences* in OLR considered here.

The mechanism behind the changes in area-averaged tropical Pacific OLR is not a simple one. Figures 2 and 3 make this point for total- and clear-sky data respectively, by comparing a sample of model results with observations in latitude-longitude space. As noted by Chou, the observed total-sky Δ(OLR) consists of both positive and negative values in the tropical Pacific domain (Fig. 2, top left). Observed OLR was less during the El Niño in the central and eastern equatorial Pacific, but it was greater during the El Niño at ~20°N and in the western equatorial Pacific. Chou showed that these changes in OLR were associated with changes in cloudiness as equatorial convection shifted eastward and the Northern Hemisphere Hadley circulation strengthened during the 1987 El Niño. Cancellation of positive and negative values of Δ(OLR), with magnitudes approaching 70 W m^{-2}, results in an area-averaged observed value of about 7 W m^{-2}.

In the models, the same qualitative pattern of total-sky Δ(OLR) also leads to extensive cancellation of positive and negative values in area-averaging. The top right portion of Figure 2 shows a longitude-latitude map of an average over the models (restricted to the 13 models for which clear-sky data was also available, to facilitate comparison with Figure 3). The average over models shows the same pattern observed by ERBE: enhanced El Niño OLR in the subtropics and the western equatorial Pacific, and reduced El Niño OLR in the central and eastern equatorial Pacific. (In fact, each of the individual models examined captures this qualitative pattern, though it is rather distorted in the extreme "outlier" models.) The magnitudes of both positive and negative Δ(OLR) are generally less than observed. Results from the two particular models whose area average total-sky Δ(OLR) was closest to that observed are shown in the bottom two frames of Figure 2. For one of these two models, ECMWF, the magnitudes of positive and negative Δ(OLR) are substantially greater than observed. In a root-mean-square sense the "average" model probably agrees better with the observations. For the other of the two models shown, CSU, agreement with observations is good in both an area-mean and root-mean-square sense.

Similar comments apply to clear-sky data, shown in Figure 3. Both observed and model-simulated quantities exhibit the general spatial pattern of positive and negative Δ(OLR) values described above for total-sky data. Again the average over models shows more muted positive and negative extremes than observed, and a smaller residual area-averaged value than observed. The two particular models whose area-average clear-sky Δ(OLR) was closest to that observed, MPI and UKMO, both obtain extremes of positive and negative values that are substantially greater in magnitude than observed.

Since in all cases the area-mean Δ(OLR) values are relatively small residuals of large positive and negative numbers, one must wonder about the sensitivity of these averages to the choice of area over which the average is taken. The middle columns in the Table address this question. In the second column, the averaging for total-sky Δ(OLR) encompasses a slightly extended area, covering 5° more latitude on both the northern and southern boundaries and 5° more longitude on both the eastern and western boundaries. The area means for both models and observations are indeed sensitive to this extension, but they generally change by the same amount. As shown in the last two lines of the Table, the observed Δ(OLR) decreases by 26% while the model-average Δ(OLR) decreases by 22%. Thus the ratio of observed to modeled Δ(OLR) remains at about 2. As shown in the third column, this ratio is preserved even when the averaging area is extended to include the tropical Atlantic. The Δ(OLR) values in this case are about half those obtained in the "default" area-averaging, but the observed number is still about twice that simulated by an average model.

3. Discussion

In exploring OLR changes and surface temperature changes between El Niño and non-El Niño times, Chou (1994) added to an observational data base that has often been used to infer Earth's climate sensitivity. Earlier work correlated OLR variations in latitude, longitude, and season with corresponding surface temperature variations (Warren and Schneider, 1979; Raval and Ramanathan, 1989; Rind et al., 1991). These earlier studies revealed strong correlation between Δ(OLR) and Δ(SST) with a slope in the neighborhood of 2 W m^{-2} K^{-1}. (Data associated with high surface temperatures in a limited area of the tropics is an exception to this rule: see Ramanathan and Collins, 1991.) Dividing this number into 4 W m^{-2}, the infrared trapping that would arise from an instantaneous doubling of atmospheric carbon dioxide, gives 2 K. As noted in the Introduction, this simple arithmetic has long been cited to interpret GCM estimates of globally averaged equilibrium warming due to doubled CO_2 (e.g., Hansen et al., 1981). Chou's data, however, imply that in the tropics Δ(OLR) / Δ(SST) ~ 7 W m^{-2} / 0.3 K, an order of magnitude larger than that obtained in the earlier studies. On its face this result implies a climate sensitivity an order of magnitude smaller than conventional wisdom would claim, at least in the tropics.

Of course there is no guarantee that any regional correlation of Δ(OLR) with Δ(SST) is a reliable indicator of Earth's response to globally averaged climate forcing such as increased atmospheric CO_2. Sun and Lindzen (1993) argued that comparison of individual points, or individual latitudes, with each other mainly reveals differences between the rising and sinking branches of the Hadley circulation. Analogous caveats apply to the interpretation of Chou's work. El Niño years are characterized by changes in horizontal SST gradients and a strengthened Hadley circulation (Pan and Oort, 1983); these phenomena may not be good proxies for global warming scenarios. For example, the GISS GCM predicts drying and enhanced OLR in the subtropics during El Niño years, consistent with the "average model" results shown in Figures 2-3. If it is forced by a globally uniform increase in either SST or atmospheric CO_2, however, the GISS model responds in the opposite way. Absolute humidity increases, trapping more longwave radiation (A. D. Del Genio, personal communication). An imposed globally uniform increase in SST was used by Cess et al. (1989) to diagnose GCM behavior. Such an experiment provides a more direct measure of a model's global climate sensitivity than the regional SST anomaly considered here, albeit at a price: one can no longer directly compare the model's response with observations.

Despite these cautionary notes, it is striking that virtually all of the AMIP models obtain changes in area-averaged tropical Pacific OLR that are substantially less than the observed values (and that this difference is maintained even when the averaging is extended well beyond the tropical Pacific). The GCMs' area-averaged total-sky Δ(OLR) is typically greater than expected for a simple blackbody model, $4\sigma T^3 \times (0.3\ K) \sim 1\text{-}2\ K$, but it is not large enough to match observations. The direction of the bias means that the GCMs are underestimating the ability of the tropical atmosphere to reject excess heat to space. Such an effect is consistent with paleo-data that implies GCMs overestimate climate sensitivity in the tropics (see Covey et al., 1996, for a brief review). Of course a complete look at climate sensitivity must include shortwave as well as longwave radiation. Chou found that the (April 1987 - April 1985) area-mean difference in absorbed solar energy over the tropical Pacific was about 3 W m^{-2}. Following the interpretation of the longwave radiation changes, the increase in absorbed shortwave during El Niño implies a positive albedo feedback that partially cancels the negative feedback implied by ΔOLR ~ 7 W m^{-2}. The models turn out to underestimate the change in area-mean absorbed solar energy by 1-2 W m^{-2} on average, at the same time that (as shown in Table 1) they underestimate ΔOLR by 3-4 W m^{-2} on average. It thus appears that partial cancellation may occur in longwave and shortwave errors relevant to climate sensitivity.

It is beyond the scope of this brief Note to elucidate the mechanisms behind the models' behavior. Some preliminary remarks follow, however, from comparing the total- and clear-sky data. Consider only the 13 models in Table 1 for which clear-sky output is available. The average, over the models, of area-mean Δ(OLR) is about 30% less than observed for *both* total- and clear-sky data. Also for these 13 models, the correlation between total- and clear-sky area-averaged Δ(OLR) is 0.96. Even though changes in OLR during El Niño years are associated with shifts in cloudiness, the source of model errors may involve clear-sky processes as well.

Acknowledgments. I am grateful to R. S. Lindzen for drawing my attention to Chou's observations, and to Mike Blackburn, Larry Gates, Marty Hoffert, Erich Roeckner and Karl Taylor for comments on the manuscript. Data processing and graphics were accomplished with the Visualization and Computation System and associated software, written by Bob Drach, Bob Mobley, Karl Taylor and Dean Williams. This work was performed under auspices of the U. S. Department of Energy by the Lawrence Livermore National Laboratory under Contract No. W-7405-Eng-48.

REFERENCES

Barkstrom, B. R., 1984: The Earth Radiation Budget Experiment (ERBE). *Bull. Amer. Meteor. Soc.*, **65**, 1170-1185.

Cess, R. D., G. L. Potter, J. P. Blanchet, G. J. Boer, S. J. Ghan, J. T. Kiehl, H. Le Treut, Z.-X. Liang, J. F. B. Mitchell, J.-J. Morcrette, D. A. Randall, M. R. Riches, E. Roeckner, U. Schlese, A. Slingo, K. E. Taylor, W. M. Washington, R. T. Weatherald, and I. Yagai, 1989: Interpretation of cloud-climate feedback as produced by 14 atmospheric general circulation models, *Science*, **245**, 513–516.

Chou, M.-D., 1994: Coolness in the tropical Pacific during an El Niño episode. *J. Climate*, **7**, 1684–1692.

Covey, C., L. C. Sloan, and M. I. Hoffert, 1996: Paleoclimate data constraints on climate sensitivity: The paleocalibration method, *Climatic Change*, in press.

Gates, W. L., 1992: AMIP: The Atmospheric Model Intercomparison Project, *Bull. Amer. Met. Soc.*, **73**, 1962–1970.

Hansen, J., D. Johnson, A. Lacis, S. Lebedeff, P. Lee, D. Rind, and G. Russell, 1981: Climatic impact of increasing atmospheric carbon dioxide, *Science*, **213**, 957–966.

Houghton, J. T., G. J. Jenkins, and J. J. Ephraums (eds.), 1990: *Climate Change: The IPCC Scientific Assessment*, Cambridge University Press, Cambridge.

Lindzen, R. S., 1990: Some coolness concerning global warming. *Bull. Amer. Meteor. Soc.*, **71**, 288–299.

Lindzen, R. S., 1994: Climate dynamics and global change. *Ann. Rev. Fluid Mech.*, **26**, 353–378.

Pan, Y. H., and A. H. Oort, 1983: Global climate variations connected with sea surface temperature anomalies in the eastern equatorial Pacific Ocean for the 1958-1973 period, *Month. Weath. Rev.*, **111**, 1244–1258.

Phillips, T. J., 1994: *A Summary Documentation of the AMIP Models*, PCMDI Report No. 18, Program for Climate Diagnosis and Intercomparison, LLNL, Livermore, CA.

Potter, G. L., and M. Fiorino, 1995: The Atmospheric Model Intercomparison Project (AMIP) diagnostic subproject on cloud radiative forcing, in *Proceedings of the First International AMIP Conference* (15–19 May 1995, Monterey, CA), WCRP-92, WMO/TD-No. 732, World Meteorological Organization, Geneva, in press.

Raval, A., and V. Ramanathan, 1989: Observational determination of the greenhouse effect, *Nature* **342**, 758–762.

Ramanathan, V., and W. Collins, 1991: Thermodynamic regulation of ocean warming by cirrus clouds deduced from observations of the 1987 El Niño, *Nature* **351**, 27–32.

Rind, D., E.-W. Chiou, W. Chu, J. Larsen, S. Oltmans, J. Lerner, M. P. McCormick, and L. McMaster, 1991: Positive water vapor feedback in climate models confirmed by satellite data, *Nature* **349**, 500–503.

Sun, D.-Z., and R. S. Lindzen, 1993: Distribution of tropical tropospheric water vapor, *J. Atmos. Sci.* **50**, 1644–1659.

Warren, S. G., and S. H. Schneider, 1979: Seasonal simulation as a test for uncertainties in the parameterizations of a Budyko-Sellers zonal climate model, *J. Atmos. Sci.* **36**, 1377–1391.

Table 1: April 1987 Minus April 1985 OLR, Averaged over the Tropics

Model Name[a]	Total-Sky Δ(OLR) [W / m²] default area[b]	extended area[c]	including Atlantic[d]	Clear-Sky Δ(OLR) [W / m²] default area[b]
BMRC	2.94	2.95	-0.46	1.49
CCC	2.02	1.53	1.04	
CNRM	5.43	4.47	3.61	
COLA	3.17	2.71	1.38	
CSIRO	3.67	2.22	2.83	1.46
CSU	6.22	5.89	2.96	1.76
DERF	3.07	2.10	0.77	1.15
DNM	1.51	1.06	0.83	
ECMWF	5.99	3.85	0.89	
GFDL	3.45	2.65	0.50	2.26
GISS	3.67	2.65	0.98	1.92
GLA	2.90	2.32	1.81	
GSFC	2.21	0.97	-0.25	
IAP	1.81	1.59	1.12	
JMA	5.41	5.13	2.96	
LMD	0.42	0.46	1.48	0.72
MGO	1.79	1.15	-0.39	
MPI	5.45	5.11	3.04	3.58
MRI	0.06	0.10	-0.39	
NCAR	2.17	2.33	2.60	1.31
NMC	2.49	2.29	1.51	1.43
NRL	-3.55	-5.08	-4.22	
SUNYA	5.10	3.19	4.56	
SUNY/GENESIS	6.18	4.45	4.03	3.95
UCLA	1.63	1.18	0.27	
UGAMP	14.02	11.43	9.15	5.28
UIUC	2.39	2.29	1.34	
UKMO	5.97	4.49	2.16	3.37
YONU	2.17	1.97	1.43	
Model Average	3.44[e]	2.67	1.64	2.28
ERBE (*observed*)	7.03	5.21	3.28	3.19

[a]See Phillips (1994) for extensive model descriptions.

[b]30°S-30°N, 100°E-100°W

[c]35°S-35°N, 95°E-95°W

[d]35°S-35°N, 95°E-0°

[e]Average over models for which clear-sky output is available = 4.55 W m^{-2}.

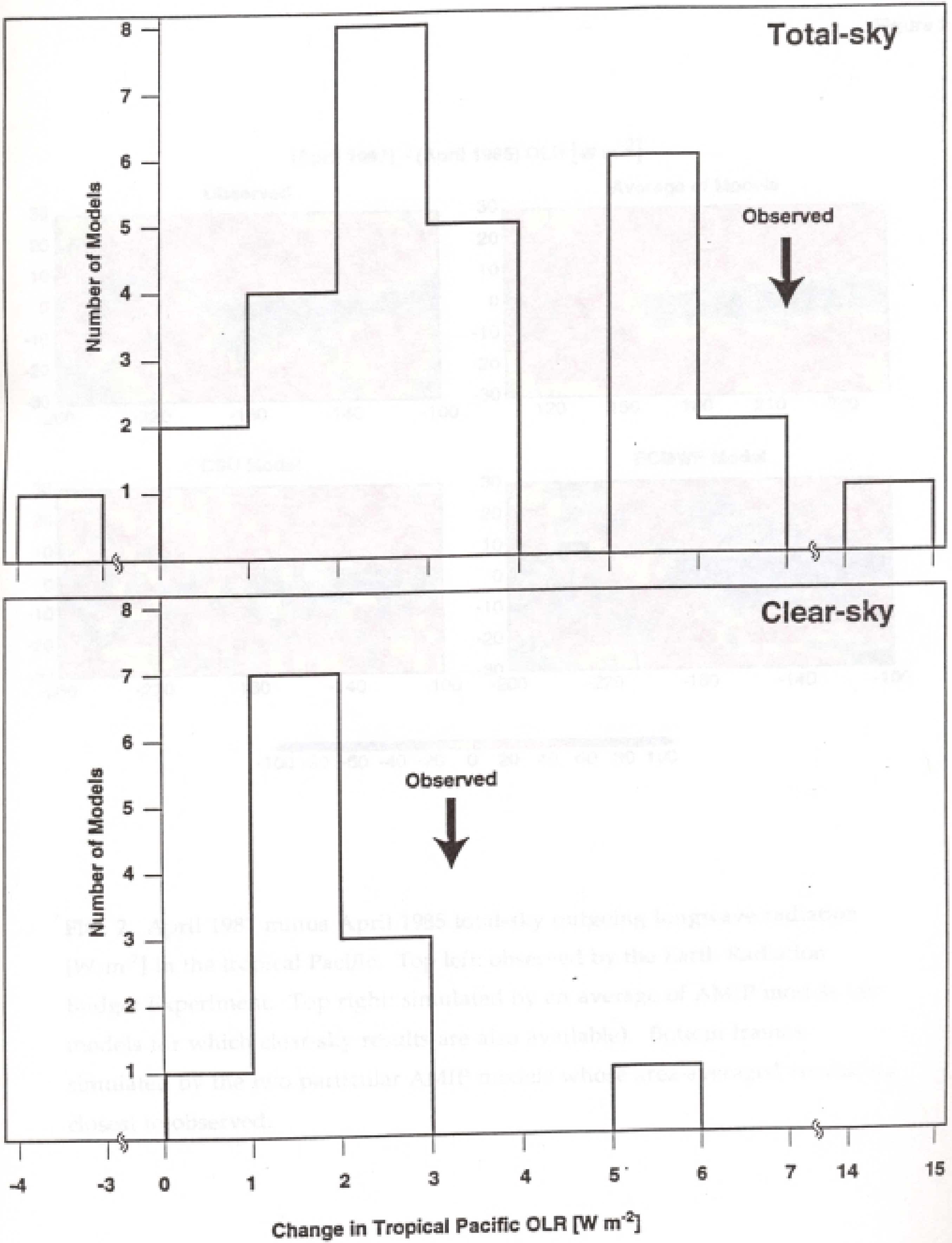

FIG. 1. Histogram of the results given in the first and last columns of Table 1.

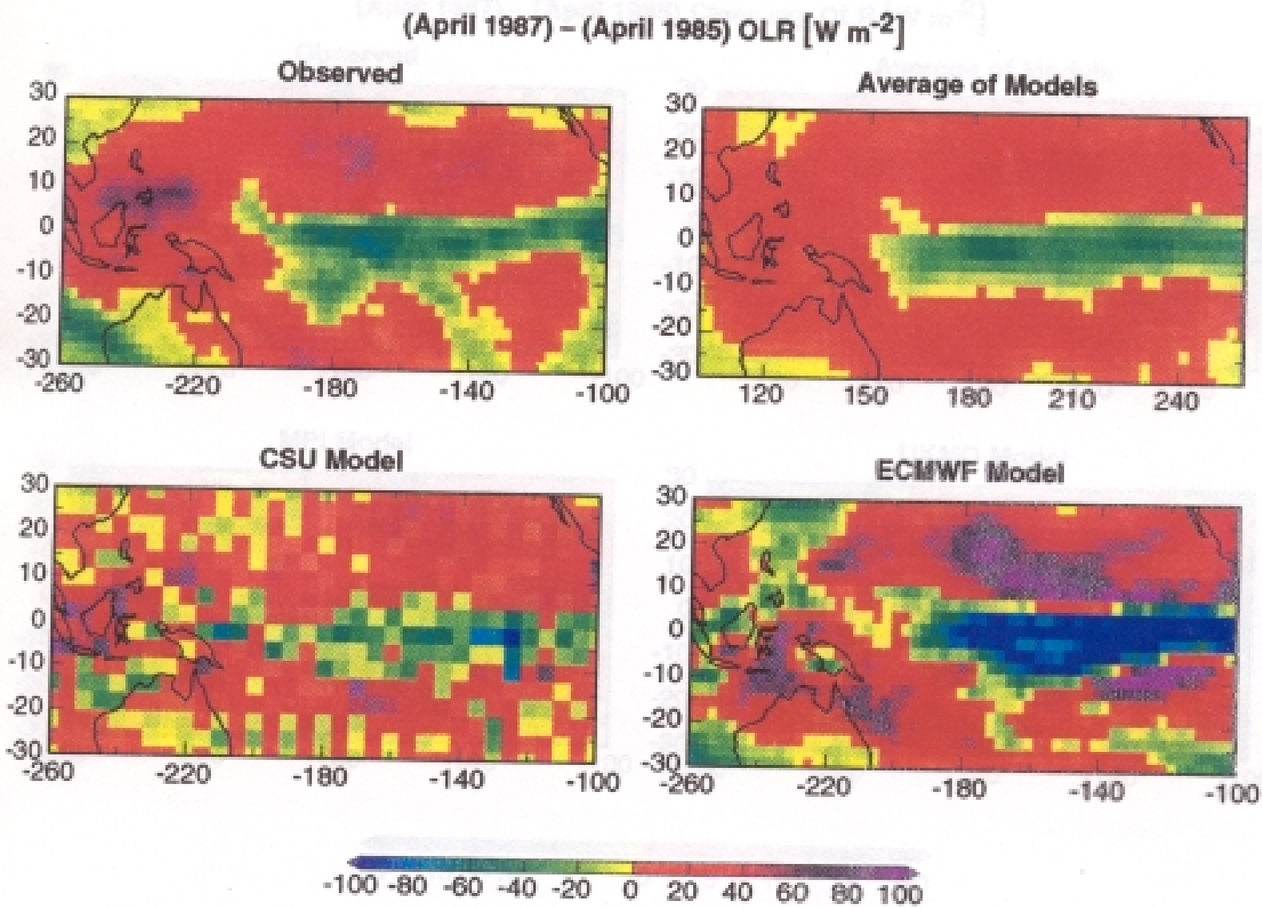

FIG. 2. April 1987 minus April 1985 total-sky outgoing longwave radiation [W m^{-2}] in the tropical Pacific. Top left: observed by the Earth Radiation Budget Experiment. Top right: simulated by an average of AMIP models (all models for which clear-sky results are also available). Bottom frames: simulated by the two particular AMIP models whose area-averaged results are closest to observed.

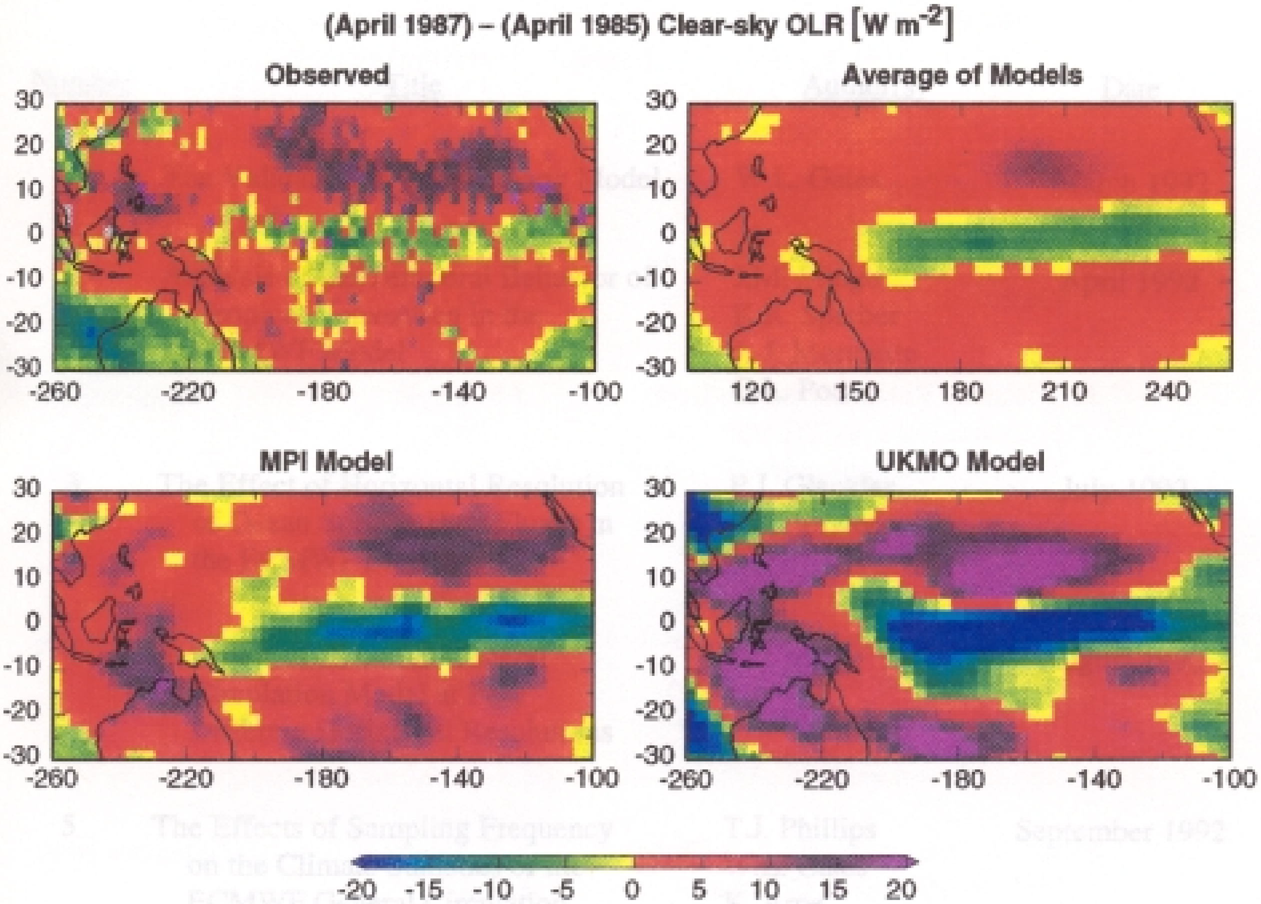

FIG. 3. Same as Fig. 2 for clear-sky outgoing longwave radiation (note the change in color scale).